

E3-2003-88

J. Honzátko¹, V. A. Khitrov², C. Pantelev²,
A. M. Sukhovoij², I. Tomandl¹

INTENSE TWO-STEP CASCADES
AND γ -DECAY SCHEME
OF THE ^{118}Sn COMPOUND NUCLEUS

Submitted to «Fizika B»

¹Nuclear Physics Institute, CZ-25068 Řež near Prague, Czech Republic

²Frank Laboratory of Neutron Physics, Joint Institute for Nuclear
Research, 141980 Dubna, Russia

1 Introduction

Both understanding of the processes occurring in a nucleus and precise calculation of important for practice parameters of these processes (for example, neutron cross-sections) requires their detailed experimental study in the wide excitation energy interval and in the large mass range of nuclei.

In these frameworks, the two-step γ -cascades following thermal neutron capture in target nucleus ^{117}Sn have been studied. The energies of γ -transitions and intensities of most strong 454 cascades exciting 303 levels in the compound nucleus were determined in the energy interval practically up to B_n .

2 Experiment

The experiment was performed at LWR-15 reactor in Řež [1]. The target, enriched in ^{117}Sn to more than 91%, was used in the experiment. The contribution of other Sn isotopes in the background of $\gamma - \gamma$ coincidences was very small.

The sum coincidence spectrum of the two-step cascades measured in the experiment is presented in Fig. 1. Using this spectrum, intensity distributions for the cascades terminating at 8 low-lying levels with $E_f < 2.8$ MeV of ^{118}Sn were built. Each two-step cascade in such spectrum is presented by a pair of peaks with equal [2] areas and widths. Energy resolutions in each of these distributions is varying from 1.9 keV at their ends to 3 keV in centre. Such a resolution at the achieved statistics of coincidences, low and practically constant at any energy background in these spectra, provided the detection threshold $\simeq 0.6 \times 10^{-4}$ events per decay for the cascades to the ground state and $2 \div 5 \times 10^{-4}$ events per decay for the cascades at the higher-lying levels.

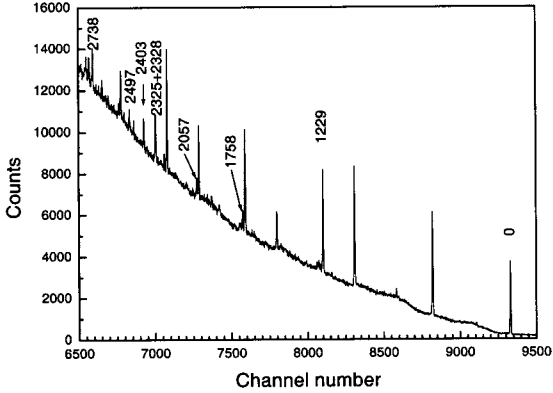


Fig. 1. The part of the sum coincidence spectrum for the target enriched in ^{117}Sn . Full energy peaks are labelled with the energy (in keV) of final cascade levels

The spectrum in Fig. 1 is very specific as compared with those for other nuclei, studied by us earlier. It has single-escape and double-escape peaks corresponding not only to one cascade transition but also to both transitions simultaneously. Thus, cascades to the ground and first excited states of ^{118}Sn create in the sum coincidence spectrum four well-expressed additional peaks shifted by 511 keV.

3 Decay scheme

The confidence of the data on peculiarities of the nuclear excited states determining intensities of the observed two-step cascades is provided, first of all, by the reliability and completeness of the obtained scheme of γ -decay. Two-step cascades following neutron capture unambiguously set energies of the initial and final levels but do not contain direct information on the energy of their intermediate level. However, if cascade is intense enough ($i_{\gamma\gamma} \geq 10^{-4}$ events per decay) then it is usually observed as a pair of the resolved peaks. In this case one can determine the quanta ordering in cascade.

The method to construct a decay scheme using obvious thesis about the constancy of the energy $E_1 = B_n - E_i$ of the primary transition in the cascades with the different total energy $E_1 + E_2 = B_n - E_f = \text{const}$ was described for the first time in [3]. The method uses the multi-dimensional Gauss distribution in the framework of the maximum likelihood method in order to select probable γ -transitions with equal energy in different spectra. As it was shown in [4], the algorithm gives reliable results even at the mean error $\simeq 1$ keV in determination of the transition energies for some hundreds of cascades placed into the decay scheme. Corresponding decay scheme for ^{118}Sn is given in Table 1.

Relative intensities of most intense cascades for all 8 spectra obtained in the experiment were transformed into absolute values by normalization to the absolute intensities of their primary transitions [5] (Table 2) and branching ratios obtained in traditional manner from the mass of coincidences accumulated in the experiment. The involving of the maximal number of the most intense cascades in normalization procedure decreases its uncertainty due to correlations between them. Some notion of the values of statistical and systematic errors is given by a comparison of the sum of intensities of all cascades proceeding via the same intermediate level with the experimental intensity of their primary transitions. At the absence of systematic errors in determination of cascade intensities, the ratio $R = \sum i_{\gamma\gamma}/i_1$ should decrease when E_1 decreases. Exceeding of R over the unity gives some total uncertainties for both intensities. Besides, owing to sufficiently different backgrounds in the spectra of cascade transitions and single γ -transitions, contribution of systematic error of i_1 in this uncertainty is larger than that of $i_{\gamma\gamma}$ at least for the smallest E_1 .

The total absolute intensities $I_{\gamma\gamma} = \sum i_{\gamma\gamma}$ of cascades with a fixed sum energy (including those unresolved experimentally) obtained in this way at the detection threshold of quanta $E_\gamma > 520$ keV are listed in Table 3. Here energy interval of the cascade final levels E_f is limited by conditions of the experiment – at the higher energies E_f the ratio peak/background in the sum coincidence spectrum decreases. This does not allow one to get reliable information on the function $i_{\gamma\gamma} = f(E_1)$ for $E_f > 2 - 3$ MeV without the Compton-suppressed spectrometer.

The total intensities $I_{\gamma\gamma}$ are suitable for revealing the serious discrepancies between the experiment and model notions of level density and radiative strength functions. Results of calculation of $I_{\gamma\gamma}^{mod}$ with the use of level density model [6], model of radiative strength functions [7] for E1- transitions and strength function $k(M1)=const$ are listed in Table 3. Considerable exceeding of the experimental cascade intensities over the calculated values means that the level density really excited after the thermal neutron capture is less than predictions of model [6] and, probably, that the radiative strength functions of the primary transitions have more strong energy dependence than that predicted by model [7].

3.1 Comparison with a known decay scheme

The decay scheme of ^{118}Sn includes 454 two-step cascades proceeding via 303 intermediate levels with the excitation energy up to $\simeq (B_n - 1)$ MeV; 110 levels from them are depopulated by two or more secondary transitions. Hence, reality of these levels is confirmed with a high confidence. (The mean uncertainty in determination of the energy of the cascade quantum is 0.48 keV). Quanta ordering for 191 cascades cannot be determined within algorithm [3] because corresponding intermediate levels are depopulated only by one secondary transition. In general case, many of these cascades can have primary transition with lower energy than energy of the secondary transition. Quanta ordering in these 191 cascades was determined using the data ENDS-file [8] on the estimated decay scheme of the nucleus under study.

It should be noted that the levels 2120, 2577 and 2725 keV listed in this file were not observed in our experiment either in the sum coincidence spectrum or as the intermediate levels of other cascades. Therefore, using data [8] one should take into account that the estimated decay scheme can contain wrong levels with mistaken spin values at this and, moreover, at higher energy.

Neutron capture cross section in a target is mainly determined by the only neutron resonance with the known parameters. Therefore, one can unambiguously assign spin and parity $J^\pi = 1^+$ to the compound state of ^{118}Sn . So, levels of this nucleus excited by the cascades (see Table 1) have, most probably, both positive and negative parity and spin values in the interval 0-2. The absence in the sum coincidence spectrum of the peak corresponding to registration of the two-step cascades to level $E_f = 2280$ keV, $J^\pi = 4^+$ [8] shows that, as in nuclei studied earlier, the total intensity of cascades with one purely quadrupole transition in ^{118}Sn is less than the detection threshold of the experiment.

3.2 Fluctuations of the cascade intensities and problem of completeness of the decay scheme

According to the conventional notions, partial widths of primary transitions following decay of neutron resonance of non-magic nucleus are the random values whose fluctuations with respect to the average obey the Porter-Thomas distribution [9]. Unfortunately, this notion was not verified for both primary γ -transitions to the levels with the energy about several MeV and in the region of the smallest partial widths. Hence, non-Gaussian character of the distribution of some amplitudes of the primary γ -transitions of a given multipolarity cannot be excluded. This can be due to, for example, contribution of large components of the wave function of the levels connected by corresponding transition in the matrix element of the primary γ -transition. In this case, experimental distribution of small partial widths will have less probability than it follows from model [9] owing to violation of the condition of application of the central limit theorem of the mathematical statistics.

The necessity of this question in practical solution arises at the analysis of the experimental data on the cascade intensities. Very low and rather even background in intensity distributions of the cascades to the lowest levels of the studied nucleus provides better sensitivity for the experiment on the study of coincidences relative to the traditional experiment [5] with a single detector. This problem for ^{118}Sn is more important than, for example, for deformed nuclei due to bigger number of intermediate levels, which are depopulated by the only γ -transition with the intensity exceeding registration threshold.

The presence of 191 cascades of this kind and, correspondingly, the necessity to determine energies of their intermediate levels (without using method [3]) requires one to solve the dilemma:

(a) either there are many levels at relatively low excitation energies in ^{118}Sn (for instance, $E_i < 3 - 4$ MeV), which do not manifest themselves in other reactions, and, as a consequence, level density in this nucleus is noticeably higher than even the predictions of model [6], at least, in this energy interval;

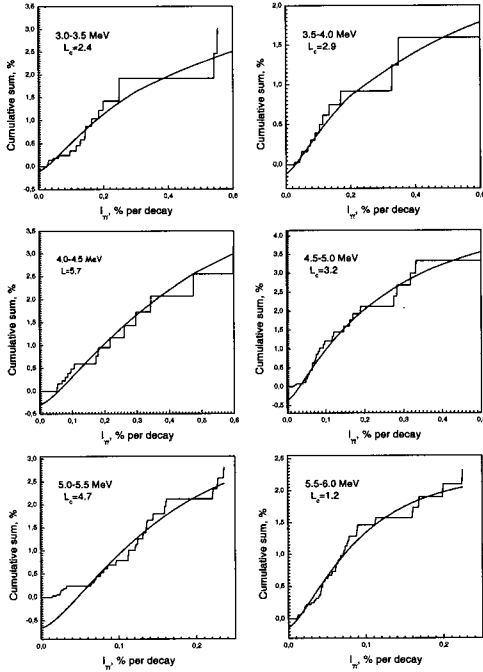


Fig. 2. Lines represent approximation and extrapolation of the cumulative intensities of cascades $i_{\gamma\gamma}$ (Table 1) in ^{118}Sn for 6 energy intervals of their intermediate levels 3.0-3.5, 4.0-4.5, 4.5-5.0, 5.0-5.5, 5.5-6.0 and 6.0-6.5 MeV versus intensity. Histogram represents the experiment. L_c is the approximated detection threshold (per 10^4 decays)

(b) or the number of primary transitions whose widths are 5-10 times smaller than the mean value is considerably less than expectation according to [9] for the same excitation energy interval.

Considerably less threshold value of the function approximating the distribution for $E_m > 5.5$ MeV in comparison with this parameter for lower energies admits only two these possible interpretations. This conclusion follows from Fig. 2, which represents the comparison between the cumulative sums of the experimental intensities of cascades proceeding via the same intermediate level (for the energy bin $\Delta E_i = 0.5$ MeV) and corresponding approximation (as it was done for the first time in [10]). Experimental data in Fig. 2 were obtained under condition that the low-intensity cascades were placed into the decay scheme in such a manner that their primary transitions have the lower energy. This assumption was used only when it was impossible to use for this aim the method [3] or data on excited levels from [8].

4 Cascades with the low-energy primary γ -transitions

Fig. 3 represents a part of the experimental intensity distribution of the cascades to the ground state of ^{118}Sn . Decay scheme of this nucleus up to $E_{ex} \geq 2.5$ MeV was very reliably established in different experiments. Based on all available data one can state to a precision of about 100% that this spectrum contains in the interval 520 to 2500 keV only 4 peaks corresponding to registration of the low-energy secondary transitions [8] of cascades. The rest of the spectrum should be related with the registration of the cascades with the energies of primary transitions $E_1 < 2.5$ MeV. The majority of the cascades with the high-energy primary transitions are usually registered in resolved intense peaks, and a number of low-intensity cascades with low-energy primary transitions form pseudo-continuous distribution in the spectrum.

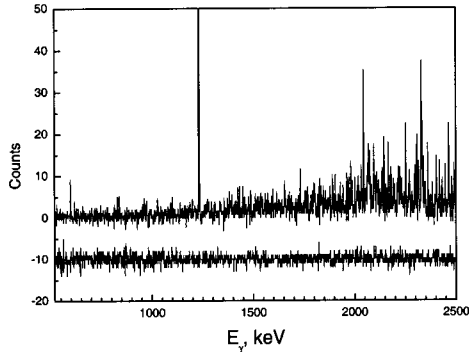


Fig. 3. The part of intensity distribution of the two-step cascades terminating at the ground state of ^{118}Sn . The background spectrum with the close sum energy presented for the comparison is shifted down by 10 counts

But observation of the resolved peak related with registration of possible low-energy primary transition of corresponding cascade permits one to get some information on structure of intermediate level of cascade. Intensity of individual cascade proceeding via a given intermediate level:

$$i_{\gamma\gamma} = i_1 \times i_2 / \sum i_2 \quad (1)$$

is always less than the intensity of its primary transition i_1 because the branching ratio $b_r = i_2 / \sum i_2$ cannot be greater than the unity. Unfortunately, background under the peaks in the sum coincidence spectrum increases when the total energy of cascade $E_1 + E_2$ decreases. This makes impossible the extraction of the main part of the secondary transition intensities at the decay of any high-energy enough intermediate level and, as a consequence, to determine i_1 as a sum of all values $i_{\gamma\gamma}$ for a given intermediate level. But for some probable primary transitions one can select from [5] close on the energy γ -quantum (which in many cases was not placed into the decay scheme suggested by authors or placed in such a manner that it was not observed in corresponding distribution of the cascade intensities). Radiative strength functions determined for such cases can be compared with the predictions of model [7]. Analysis [11], made for the experimental intensity distributions $I_{\gamma\gamma}$ of two-step cascades to the ground and first excited states of ^{118}Sn with accounting for the known total radiative width $\Gamma_\lambda = 80$ meV, shows that the radiative strength function up to the energy

$E_1 \simeq 3.5$ MeV does not exceed the value predicted by model [7]. Therefore, this model can be used for estimation of probability of low-energy primary transitions whose partial widths considerably exceed the mean value.

In this experiment have been observed, at least, 15 cascades with the most intense, low-energy primary transitions ($E_1 < 2.5$ MeV) whose partial widths are, at least, 20 times larger than the prediction of [7]. According to model [6], approximately 26000 levels are expected to be excited by the primary $E1$ and $M1$ γ -transitions in the excitation energy region from 6.5 to 8.3 MeV. The probability to observe the only random exceeding of partial width over the average by a factor of 20 and more for the considered γ -transitions in the framework of the Porter-Thomas distribution is equal to 10^{-5} .

Hence, from the above statement that some of the observed in [5] γ -transitions are really primary follows that some part of these transitions have anomalous large widths whose appearance cannot be random. Therefore, some of the levels with the excitation energy ≥ 6 MeV must considerably differ in the structure of the wave functions from the neighbouring levels. I. e., the effects like those observed at the low excitation energy manifest themselves and at higher excitations.

The presence of very intense low-energy primary γ -transitions was established earlier [12] in the $^{126,127,129,131}\text{Te}$ compound nuclei. They are interpreted as direct capture of neutron at the sub-shells $3P_{3/2}$ and $3P_{1/2}$. Unfortunately, clarifying of possible structure of the considered levels of ^{118}Sn is impossible without further experimental and theoretical investigations.

5 Possible regularity of the excitation spectrum of the intermediate levels of the most intense cascades

According to the modern theoretical notions, the wave function structure of any excited states is determined by co-existence and interaction between the fermion (quasi-particles) and boson (phonons) excitations. With the excitation energy a nucleus transits from practically mono-component excitations of the mentioned types to the mixed (quasi-particles \otimes phonons) states with rather different [13] degree of their fragmentation. This process should be investigated in details but there is no adequate experimental methods to study the structure of the wave functions, at least, up to the excitation energy not less than 5 MeV.

Nevertheless, some information on the probable dominant components of wave functions of heavy deformed nuclei can be obtained even in this case. The authors of [14] suggested to search for the regularity in the excitation spectra of the intermediate levels of the most intense cascades by means of auto-correlation analysis of the smoothed distributions of the sum cascade intensities from Table 1. Intensities were smoothed by means of the Gaussian function: $F(E) = \sum i_{\gamma\gamma} \times \exp(-0.5(\Delta E/\sigma)^2)$. The distribution of this type smoothed with the parameter $\sigma = 25$ keV is given in Fig. 4, and the values of the auto-correlation function

$$A(T) = \sum_E F(E) \times F(E + T) \times F(E + 2T) \quad (2)$$

for different selection thresholds of intense cascades are shown in Fig. 5. As it was shown in [15], such an analysis cannot give unique value of the equidistant period T even for the simulated spectra (for example, for 25 “bands” consisting from 4 levels with slightly distorted equidistant period and intensities of cascades) and provide estimation of the confidence level of the observed effect. In principle, both problems can be solved in the experiments on the study of the two-step cascades in different resonances of the same nucleus. But some grounds to state that the regularity really exists can be obtained from a comparison of the most probable equidistant periods in different nuclei. The set of the probable equidistant periods obtained so far (Fig. 6) allows an assumption that the T value is approximately proportional to the number of boson pairs of the unfilled nuclear shells. This allows one to consider the effect at the level of working hypothesis, though the probability of random existence of the regular spectrum of intermediate levels of the most intense cascades in each, arbitrary nucleus cannot be equal to zero. The regularity in the excitation spectra testifies to the harmonic nuclear vibrations. Thus, one can assume that the structure of the intermediate levels of the studied cascades contains considerable components of the rather weakly fragmented states like multi-quasi-particle excitations \otimes phonon or several phonons. This provides logical explanation of serious decrease in the observed level density as compared with the predictions of the non-interacting Fermi-gas model: nuclear excitation energy concentrates on phonons but quasi-particle states in the energy interval up to $\simeq 2$ MeV are excited weakly or very weakly due to insufficiency of energy for

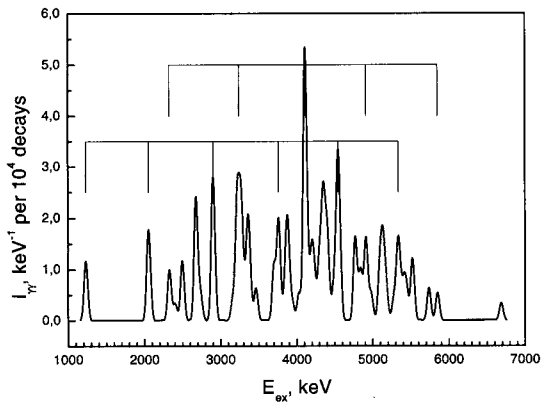


Fig. 4. The dependence of the “smoothed” intensities of resolved cascades listed in Table 1 on the excitation energy. Possible “bands” of practically harmonic excitations of the nucleus are marked. The parameter $\sigma = 25$ keV was used

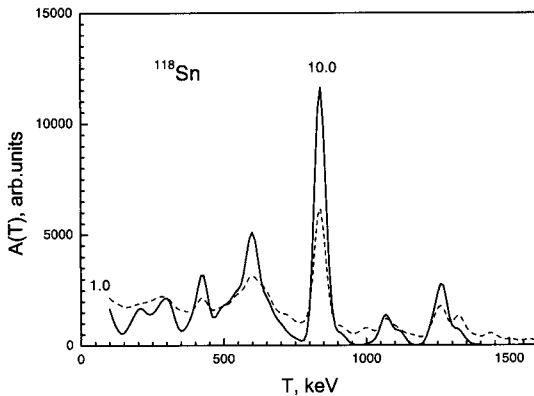


Fig. 5. The values of the functional $A(T)$ for two registration thresholds of most intense cascades. The value of the registration threshold (per 10^4 decays) is given in the figure

breaking of paired nucleons. This is quite probable but, in principle, not the only explanation.

6 Cascade population of levels in ^{118}Sn .

Obvious deviations of level density and radiative strength functions from predictions of from the simplest models like [6,7] and probable regularity in the excitation spectra of intermediate levels of the most intense cascades show that the notions of the cascade γ -decay process need development and some corrections. This necessity follows from a comparison between the experimental and model calculated values of the population of the high-lying levels of the nucleus under study. It is seen from eq. (1) that at the presence of reliable information on the intensities of individual cascades and known [5] intensities of their primary and secondary transitions one can to determine $\sum i_2$, which equals the total population of a given level by the direct primary transitions and any possible cascades. It is worthwhile to subtract the primary transition intensity from this value in order to decrease its fluctuation. The populations obtained in this manner for the levels with positive parity are compared with the model calculated values in Fig. 7. It should be noted that difference between the calculated populations of levels with the same spin but different parities is insignificant. It is seen that the correspondence between the experiment and calculation for the levels above ≈ 3 MeV cannot be achieved. On the one side, this result confirms the conclusion made above on the presence of the excitation energy interval where occurs principle change in properties of the excited states of not only deformed but also spherical nuclei and, on the other side, it points at the necessity to develop more precise nuclear models for the all interval of the excitation energies $E_m \simeq B_n$.

7 Conclusion

For the first time, the large enough and reliable scheme of the excited states and modes of their decay for the ^{118}Sn compound nucleus were obtained in the experiment with the excitation energy more than 3 MeV.

Analysis of this information shows, in particular, that an improvement of precision in description of properties of spherical nucleus requires more detailed accounting for co-existence and interaction of quasi-particle and phonon components of wave functions of the levels excited after the neutron capture.

This work was supported by GACR under contract No. 202/03/0891 and by RFBR Grant No. 99-02-17863.

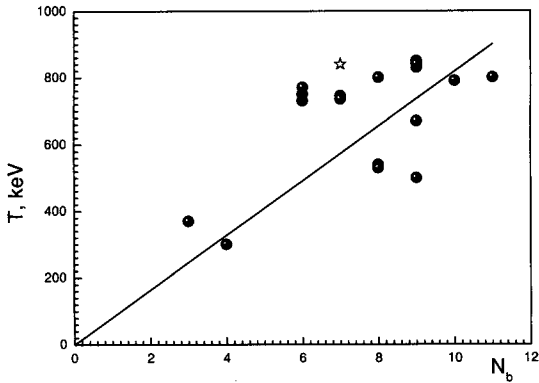


Fig. 6. The value of the equidistant period T for ^{118}Sn (asterisk) and other investigated even-even nuclei as a function of the number of boson pairs N_b in the unfilled shells. The line represents possible dependence (drawn by eye)

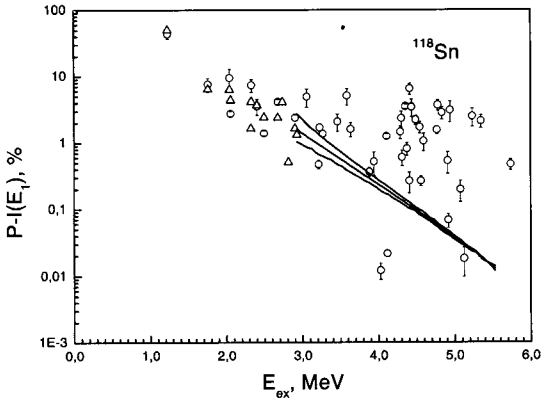


Fig. 7. Experimental population of different levels in ^{118}Sn (points with bars) in comparison with that calculated for levels $J^\pi = 0^+, 1^+, 2^+$ within models [6] and [7] using $k(M1) = \text{const}$ - curves and triangles

Table 1.

A list of absolute intensities (per 10^2 decays), $i_{\gamma\gamma}$, of measured two-step cascades and energies, E_1 and E_2 , of the cascade transitions, E_i is the energy of the intermediate levels

E_1, keV	E_i, keV	E_2, keV	$i_{\gamma\gamma}$	E_1, keV	E_i, keV	E_2, keV	$i_{\gamma\gamma}$
8095.5	1230.8(1)	1230.8	0.366(18)	5972.3	3354.0(3)	2124.3	0.168(16)
7567.3	1759.0(1)	529.3	0.026(4)			1311.1	0.017(3)
7282.4	2043.9(3)	2043.9	0.054(8)	5969.8	3356.5(2)	3356.5	0.053(8)
		814.2	0.075(7)			2126.8	0.182(16)
7268.2	2058.1(1)	828.4	0.444(13)			1313.6	0.014(3)
6997.4	2328.9(3)	2328.9	0.069(10)	5961.3	3365.0(1)	3365.0	0.096(12)
		1099.2	0.243(13)	5951.3	3375.0(12)	3375.0	0.058(8)
6922.9	2403.4(9)	2403.4	0.024(5)			2145.3	0.029(7)
		1173.7	0.104(8)			1049.1	0.056(9)
6828.1	2498.2(1)	1268.5	0.366(13)	5944.2	3382.1(1)	3382.1	0.163(15)
6750.6	2575.7(6)	2575.7	0.013(5)	5900.3	3426.0(3)	1100.1	0.029(8)
6747.2	2579.1(3)	2579.1	0.024(7)	5866.7	3459.6(4)	1133.7	0.025(9)
6648.3	2678.0(2)	2678.0	0.365(24)	5862.5	3463.8(7)	3463.8	0.056(8)
		1448.3	0.350(11)			2234.1	0.032(7)
		919.7	0.030(5)			1420.9	0.055(4)
6587.4	2738.9(3)	2738.9	0.051(8)			1137.9	0.057(9)
		1509.2	0.104(8)	5813.2	3513.1(3)	3513.1	0.018(5)
6421.5	2904.8(2)	2904.8	0.646(39)			2283.4	0.024(7)
		1675.1	0.217(11)	5739.7	3586.6(2)	1260.7	0.026(7)
		861.9	0.014(3)	5724.5	3601.8(3)	3601.8	0.048(7)
6268.3	3058.0(3)	3058.0	0.029(7)			2372.1	0.020(7)
6192.2	3134.1(3)	1904.4	0.026(7)	5688.6	3637.7(5)	3637.7	0.029(7)
6188.2	3138.1(1)	1908.4	0.044(7)			1311.8	0.047(6)
6167.5	3158.8(1)	3158.8	0.128(13)	5630.2	3696.1(2)	2466.4	0.046(8)
6110.3	3216.0(11)	3216.0	0.098(12)	5626.3	3700.0(6)	3700.0	0.037(7)
		1986.3	0.164(13)			2470.3	0.038(8)
		1173.1	0.122(8)			1374.1	0.129(8)
		890.1	0.158(12)			962.0	0.123(10)
6096.5	3229.8(8)	3229.8	0.214(18)	5563.3	3763.0(3)	2533.3	0.494(23)
		2000.1	0.034(7)			1720.1	0.046(4)
6065.6	3260.7(1)	3260.7	0.144(15)			1437.1	0.073(7)
6055.2	3271.1(1)	3271.1	0.552(28)	5478.6	3847.7(6)	3847.7	0.038(7)
6052.4	3273.9(2)	2044.2	0.031(7)			2618.0	0.031(10)
6016.6	3309.7(6)	3309.7	0.021(5)			1521.8	0.046(7)
		2080.0	0.070(8)	5469.1	3857.2(3)	3857.2	0.106(12)
		906.5	0.024(142)			2627.5	0.028(10)
5986.1	3340.2(4)	3340.2	0.037(8)	5459.8	3866.5(6)	2636.8	0.041(10)
		2110.5	0.024(7)			1540.6	0.049(7)

E_1, keV	E_i, keV	E_2, keV	$i_{\gamma\gamma}$
5443.0	3883.3(1)	1557.4	0.349(13)
5436.9	3889.4(1)	3889.4	0.170(15)
5382.0	3944.3(4)	3944.3	0.056(8)
		2714.6	0.047(11)
5330.7	3995.6(3)	2765.9	0.031(10)
		1952.7	0.018(3)
5297.1	4029.2(1)	1291.2	0.174(9)
5280.9	4045.4(2)	2815.7	0.078(13)
5216.9	4109.4(5)	2879.7	0.586(31)
		2066.5	0.013(3)
5208.6	4117.7(2)	4117.7	0.445(24)
		2888.0	0.635(31)
		2074.8	0.009(3)
5193.1	4133.2(3)	4133.2	0.062(10)
		2903.5	0.024(10)
5134.9	4191.4(6)	4191.4	0.016(5)
		2961.7	0.259(20)
		1865.5	0.069(7)
5099.3	4227.0(3)	4227.0	0.080(12)
		2997.3	0.217(22)
5037.9	4288.4(1)	3058.7	0.181(20)
5025.3	4301.0(3)	4301.0	0.024(7)
		3071.3	0.044(13)
5014.1	4312.2(7)	3082.5	0.040(11)
		2269.3	0.014(3)
		1986.3	0.106(8)
		1574.2	0.102(8)
4993.3	4333.0(5)	4333.0	0.018(5)
		3103.3	0.035(11)
4972.5	4353.8(5)	4353.8	0.069(10)
		3124.1	0.395(28)
		2595.5	0.059(8)
		2310.9	0.056(5)
		2296.9	0.076(13)
4949.4	4376.9(7)	4376.9	0.011(5)
		2051.0	0.066(8)
		1638.9	0.029(8)
4922.0	4404.3(3)	4404.3	0.058(10)
		2361.4	0.038(4)
4919.0	4407.3(6)	4407.3	0.050(10)

E_1, keV	E_i, keV	E_2, keV	$i_{\gamma\gamma}$
		3177.6	0.393(30)
		2081.4	0.033(8)
4915.8	4410.5(3)	2652.2	0.027(8)
		2367.6	0.028(4)
4891.0	4435.3(4)	3205.6	0.031(11)
		2677.0	0.023(7)
4836.5	4489.8(1)	4489.8	0.218(18)
4824.7	4501.6(6)	3271.9	0.029(10)
		2743.3	0.019(8)
4789.5	4536.8(5)	4536.8	0.211(18)
		3307.1	0.038(10)
		2778.5	0.061(9)
		2493.9	0.021(4)
4781.3	4545.0(6)	4545.0	0.117(13)
		3315.3	0.037(10)
		2502.1	0.030(4)
		2488.1	0.055(11)
		2141.8	0.044(6)
4765.6	4560.7(3)	4560.7	0.174(16)
		3331.0	0.081(11)
		2802.4	0.129(12)
		2503.8	0.126(15)
4731.8	4594.5(3)	4594.5	0.030(7)
		3364.8	0.024(10)
4700.9	4625.4(2)	2568.5	0.059(11)
4685.6	4640.7(3)	2583.8	0.048(11)
4658.9	4667.4(3)	2610.5	0.040(11)
4653.7	4672.6(2)	4672.6	0.058(10)
4627.4	4698.9(4)	4698.9	0.021(7)
4614.5	4711.8(4)	4711.8	0.018(7)
4602.4	4723.9(9)	4723.9	0.024(7)
		3494.2	0.052(11)
		2681.0	0.009(4)
4584.3	4742.0(3)	4742.0	0.024(7)
4556.8	4769.5(6)	3539.8	0.028(8)
		2443.6	0.122(11)
		2366.3	0.126(10)
4553.5	4772.8(5)	4772.8	0.034(8)
		3543.1	0.035(8)
		2729.9	0.017(4)

E_1, keV	E_i, keV	E_2, keV	$i_{\gamma\gamma}$
		2446.9	0.035(9)
4547.6	4778.7(3)	3020.4	0.050(8)
		2735.8	0.017(4)
		2721.8	0.049(10)
4523.4	4802.9(5)	3573.2	0.026(8)
		2760.0	0.011(4)
		2477.0	0.029(9)
4509.6	4816.7(5)	3058.4	0.031(8)
		2078.7	0.034(10)
4496.7	4829.6(1)	4829.6	0.098(13)
4492.0	4834.3(6)	3604.6	0.063(10)
		2508.4	0.084(11)
4482.0	4844.3(2)	4844.3	0.075(12)
4477.7	4848.6(3)	4848.6	0.013(5)
		3618.9	0.029(8)
		2110.6	0.129(10)
4456.8	4869.5(5)	4869.5	0.029(8)
		3639.8	0.037(8)
4451.7	4874.6(2)	4874.6	0.094(13)
4446.7	4879.6(3)	4879.6	0.038(8)
		3121.3	0.036(8)
4432.8	4893.5(1)	4893.5	0.080(12)
4415.5	4910.8(6)	4910.8	0.011(5)
		3681.1	0.050(10)
		2584.9	0.199(15)
		2507.6	0.058(9)
4406.6	4919.7(1)	2862.8	0.190(21)
4402.9	4923.4(3)	2880.5	0.046(5)
		2520.2	0.025(8)
4384.6	4941.7(3)	2898.8	0.017(4)
		2615.8	0.036(10)
4370.5	4955.8(5)	4955.8	0.014(5)
4344.8	4981.5(2)	4981.5	0.011(5)
		3751.8	0.047(10)
		2924.6	0.066(13)
		2655.6	0.036(10)
4325.3	5001.0(3)	5001.0	0.026(7)
4295.3	5031.0(4)	5031.0	0.026(8)
4282.9	5043.4(3)	5043.4	0.014(5)
		3813.7	0.054(10)
4250.6	5075.7(3)	5075.7	0.032(8)

E_1, keV	E_i, keV	E_2, keV	$i_{\gamma\gamma}$
4248.0	5078.3(9)	5078.3	0.046(10)
		3320.0	0.030(8)
		3035.4	0.009(4)
4236.0	5090.3(4)	5090.3	0.070(10)
		3860.6	0.109(13)
		3332.0	0.015(6)
		3047.4	0.034(5)
4217.2	5109.1(5)	5109.1	0.014(5)
4206.7	5119.6(4)	5119.6	0.014(5)
		3076.7	0.031(5)
		3062.7	0.050(12)
		2793.7	0.041(13)
4201.7	5124.6(5)	3894.9	0.038(10)
		2386.6	0.093(10)
4184.5	5141.8(8)	3912.1	0.124(13)
		3383.5	0.019(8)
		2815.9	0.030(13)
		2738.6	0.049(9)
4163.5	5162.8(8)	5162.8	0.050(8)
		2836.9	0.039(13)
		2759.6	0.024(9)
4144.8	5181.5(3)	3124.6	0.065(12)
		2778.3	0.047(9)
4124.9	5201.4(9)	5201.4	0.048(8)
		3971.7	0.034(8)
		3158.5	0.015(4)
4105.8	5220.5(2)	5220.5	0.029(7)
4093.2	5233.1(3)	3190.2	0.024(4)
		3176.2	0.046(11)
4082.1	5244.2(3)	5244.2	0.045(8)
		4014.5	0.020(10)
4073.0	5253.3(4)	5253.3	0.014(5)
4064.0	5262.3(3)	5262.3	0.024(7)
4051.4	5274.9(5)	5274.9	0.102(12)
		3232.0	0.022(4)
4025.5	5300.8(4)	4071.1	0.032(10)
4003.3	5323.0(5)	5323.0	0.142(15)
		3564.7	0.043(8)
		2997.1	0.050(11)
3996.8	5329.5(3)	5329.5	0.046(8)
		4099.8	0.034(10)

E_1, keV	E_i, keV	E_2, keV	$i_{\gamma\gamma}$
3983.0	5343.3(6)	5343.3	0.093(12)
		4113.6	0.057(10)
		3300.4	0.010(4)
3978.1	5348.2(8)	4118.5	0.050(10)
		3589.9	0.025(8)
		3305.3	0.018(4)
		3022.3	0.068(11)
		3022.3	0.068(11)
3967.0	5359.3(6)	4129.6	0.020(8)
3958.9	5367.4(1)	5367.4	0.077(10)
3929.6	5396.7(5)	5396.7	0.094(12)
3917.3	5409.0(5)	3339.8	0.050(11)
		4179.3	0.024(8)
		4194.6	0.023(10)
3902.0	5424.3(7)	3666.0	0.025(8)
		3367.4	0.057(14)
3879.3	5447.0(3)	3021.1	0.030(7)
		5447.0	0.085(10)
		3121.1	0.036(11)
3823.8	5502.5(3)	5502.5	0.030(7)
		3459.6	0.011(3)
3808.8	5517.5(3)	5517.5	0.099(12)
		4287.8	0.061(10)
3801.0	5525.3(5)	5525.3	0.205(16)
		4295.6	0.020(10)
		5549.2	0.018(5)
3777.1	5549.2(11)	4319.5	0.024(10)
3767.5	5558.8(7)	4329.1	0.020(10)
3760.5	5565.8(5)	5565.8	0.013(5)
3736.7	5589.6(2)	5589.6	0.051(8)
3728.4	5597.9(1)	5597.9	0.078(10)
3712.7	5613.6(2)	5613.6	0.045(7)
3695.8	5630.5(2)	5630.5	0.030(7)
		3872.2	0.023(7)
		3587.6	0.014(3)
3655.0	5671.3(4)	5671.3	0.013(5)
3634.0	5692.3(5)	4462.6	0.021(8)
3614.1	5712.2(1)	5712.2	0.077(10)
3588.7	5737.6(8)	5737.6	0.168(13)
		3411.7	0.031(9)
3568.3	5758.0(5)	5758.0	0.019(5)
		3432.1	0.043(9)

E_1, keV	E_i, keV	E_2, keV	$i_{\gamma\gamma}$
3552.9	5773.4(2)	4543.7	0.064(10)
3535.5	5790.8(3)	5790.8	0.021(5)
3502.6	5823.7(3)	5823.7	0.016(5)
3496.3	5830.0(2)	4600.3	0.089(13)
3486.7	5839.6(7)	5839.6	0.030(7)
		4609.9	0.031(8)
3475.7	5850.6(4)	5850.6	0.051(8)
		4620.9	0.083(11)
3465.2	5861.1(3)	3807.7	0.035(4)
		4631.4	0.034(8)
		5870.2	0.018(5)
3456.1	5870.2(3)	5870.2	0.018(5)
3451.5	5874.8(2)	3831.9	0.022(4)
3448.3	5878.0(4)	3835.1	0.011(4)
3444.6	5881.7(2)	4652.0	0.073(11)
3434.2	5892.1(6)	5892.1	0.080(10)
		4662.4	0.032(10)
3428.9	5897.4(3)	5897.4	0.021(5)
3422.9	5903.4(2)	5903.4	0.056(8)
3419.0	5907.3(12)	5907.3	0.016(5)
		4677.6	0.023(8)
3407.3	5919.0(4)	5919.0	0.030(7)
3401.1	5925.2(6)	4689.3	0.041(10)
		4695.5	0.023(10)
3392.6	5933.7(6)	5933.7	0.046(8)
3387.8	5938.5(5)	4704.0	0.043(10)
		4708.8	0.029(10)
3380.2	5946.1(3)	4716.4	0.043(10)
3358.0	5968.3(4)	4738.6	0.035(10)
3351.9	5974.4(2)	5974.4	0.045(8)
3331.4	5994.9(12)	5994.9	0.035(7)
		3952.0	0.012(4)
3322.1	6004.2(2)	6004.2	0.064(10)
		4774.5	0.052(10)
3303.9	6022.4(3)	4792.7	0.054(11)
3293.4	6032.9(1)	6032.9	0.029(7)
		4803.2	0.037(10)
3284.4	6041.9(3)	4812.2	0.037(10)
3278.2	6048.1(1)	6048.1	0.016(7)
		4818.4	0.038(10)
3265.3	6061.0(3)	3722.2	0.030(9)
		6061.0	0.037(8)

E_1, keV	E_i, keV	E_2, keV	$i_{\gamma\gamma}$
3252.7	6073.6(4)	6073.6	0.019(7)
3245.5	6080.8(1)	6080.8	0.062(10)
		4851.1	0.026(10)
3229.4	6096.9(5)	4867.2	0.028(10)
3225.0	6101.3(3)	6101.3	0.026(7)
3204.7	6121.6(3)	6121.6	0.029(7)
3180.5	6145.8(2)	6145.8	0.054(10)
3172.6	6153.7(5)	4924.0	0.034(11)
3168.0	6158.3(2)	4928.6	0.067(13)
3150.4	6175.9(6)	4946.2	0.028(11)
3142.6	6183.7(2)	6183.7	0.061(10)
3135.9	6190.4(5)	6190.4	0.014(5)
3123.1	6203.2(3)	6203.2	0.032(7)
3113.0	6213.3(3)	6213.3	0.026(7)
3083.6	6242.7(3)	6242.7	0.019(5)
3073.6	6252.7(1)	6252.7	0.061(10)
3066.0	6260.3(2)	6260.3	0.038(8)
3059.2	6267.1(5)	4224.2	0.011(4)
3054.0	6272.3(4)	6272.3	0.016(5)
3044.4	6281.9(1)	6281.9	0.021(8)
		5052.2	0.050(13)
3041.6	6284.7(3)	6284.7	0.029(8)
3029.2	6297.1(3)	6297.1	0.021(7)
3021.7	6304.6(1)	6304.6	0.038(8)
		4261.7	0.050(6)
2998.1	6328.2(3)	4285.3	0.018(4)
2992.7	6333.6(4)	6333.6	0.029(7)
		5103.9	0.037(11)
2982.2	6344.1(2)	6344.1	0.046(8)
2968.6	6357.7(2)	6357.7	0.038(8)
2961.7	6364.6(12)	6364.6	0.059(10)
		4606.3	0.034(8)
2951.7	6374.6(3)	6374.6	0.035(8)
2947.9	6378.4(5)	6378.4	0.018(7)
2941.6	6384.7(3)	6384.7	0.034(7)
2937.4	6388.9(4)	6388.9	0.021(7)
2921.8	6404.5(6)	6404.5	0.011(5)
2906.1	6420.2(10)	5190.5	0.040(10)
		4377.3	0.011(4)
2897.4	6428.9(4)	6428.9	0.027(8)
2890.7	6435.6(4)	4392.7	0.012(4)

E_1, keV	E_i, keV	E_2, keV	$i_{\gamma\gamma}$
2888.1	6438.2(3)	4679.9	0.030(8)
2885.5	6440.8(4)	6440.8	0.035(10)
2878.7	6447.6(3)	6447.6	0.035(10)
2873.0	6453.3(8)	6453.3	0.026(8)
		5223.6	0.058(11)
2867.6	6458.7(4)	5229.0	0.034(10)
2840.9	6485.4(3)	6485.4	0.027(7)
2829.1	6497.2(3)	6497.2	0.021(7)
2824.5	6501.8(4)	6501.8	0.016(5)
2817.3	6509.0(3)	4466.1	0.013(4)
2810.6	6515.7(4)	6515.7	0.026(7)
		5286.0	0.026(10)
2799.6	6526.7(4)	6526.7	0.013(5)
2792.9	6533.4(5)	6533.4	0.026(7)
		5303.7	0.029(10)
2788.1	6538.2(5)	6538.2	0.013(5)
2770.6	6555.7(5)	6555.7	0.016(5)
2766.9	6559.4(3)	6559.4	0.035(8)
2762.5	6563.8(5)	6563.8	0.016(5)
2753.3	6573.0(2)	6573.0	0.030(7)
2745.1	6581.2(4)	4538.3	0.011(4)
2727.7	6598.6(3)	6598.6	0.046(12)
2725.1	6601.2(4)	6601.2	0.038(12)
2704.4	6621.9(2)	6621.9	0.032(7)
2694.6	6631.7(5)	5402.0	0.026(10)
2680.0	6646.3(2)	5416.6	0.067(11)
2658.1	6668.2(4)	4265.0	0.024(8)
2640.1	6686.2(1)	6686.2	0.107(15)
2623.3	6703.0(5)	5473.3	0.028(10)
2612.9	6713.4(6)	6713.4	0.045(10)
		5483.7	0.035(10)
2609.1	6717.2(4)	6717.2	0.024(7)
2603.8	6722.5(4)	6722.5	0.016(5)
2589.9	6736.4(4)	6736.4	0.016(5)
2581.6	6744.7(4)	5515.0	0.028(8)
2574.4	6751.9(5)	4426.0	0.025(10)
2566.2	6760.1(5)	6760.1	0.013(5)
2562.3	6764.0(4)	6764.0	0.018(5)
2551.0	6775.3(12)	6775.3	0.021(5)
		4449.4	0.031(10)
2538.9	6787.4(4)	6787.4	0.014(5)

E_1, keV	E_i, keV	E_2, keV	$i_{\gamma\gamma}$
2533.2	6793.1(4)	6793.1	0.030(7)
		4750.2	0.011(3)
2526.0	6800.3(5)	6800.3	0.013(5)
2522.0	6804.3(4)	6804.3	0.018(5)
2500.6	6825.7(4)	6825.7	0.024(7)
		5596.0	0.035(8)
2497.5	6828.8(6)	5599.1	0.020(8)
2463.7	6862.6(2)	6862.6	0.038(7)
2445.8	6880.5(3)	6880.5	0.024(5)
2432.0	6894.3(6)	6894.3	0.013(5)
		5664.6	0.018(8)
2416.6	6909.7(3)	6909.7	0.014(5)
2402.2	6924.1(5)	5694.4	0.018(7)
2394.4	6931.9(3)	5702.2	0.028(7)
2382.2	6944.1(11)	6944.1	0.010(5)
		4618.2	0.027(9)
2345.0	6981.3(5)	6981.3	0.010(4)
2339.4	6986.9(3)	6986.9	0.016(5)
2333.4	6992.9(1)	6992.9	0.029(7)
		5763.2	0.021(7)
2329.9	6996.4(3)	4670.5	0.034(9)
2315.2	7011.1(3)	7011.1	0.018(5)
2312.3	7014.0(3)	4276.0	0.042(10)
2306.8	7019.5(3)	7019.5	0.030(7)
2296.0	7030.3(5)	7030.3	0.010(5)
2270.0	7056.3(4)	7056.3	0.016(5)
2251.6	7074.7(2)	7074.7	0.026(7)
2223.7	7102.6(3)	7102.6	0.013(4)
		5872.9	0.026(7)
2214.9	7111.4(8)	7111.4	0.018(5)
		4785.5	0.041(8)
2211.1	7115.2(4)	7115.2	0.011(4)
2191.1	7135.2(3)	7135.2	0.013(4)
2179.0	7147.3(3)	7147.3	0.018(5)
2164.9	7161.4(3)	7161.4	0.014(5)
2151.2	7175.1(6)	7175.1	0.010(4)

E_1, keV	E_i, keV	E_2, keV	$i_{\gamma\gamma}$
2144.1	7182.2(2)	7182.2	0.027(7)
2135.0	7191.3(3)	7191.3	0.018(5)
2127.3	7199.0(3)	5156.1	0.010(3)
2112.1	7214.2(5)	7214.2	0.010(4)
2107.9	7218.4(4)	7218.4	0.014(5)
2098.9	7227.4(4)	7227.4	0.013(5)
2094.1	7232.2(2)	7232.2	0.022(5)
2073.3	7253.0(3)	7253.0	0.026(5)
2068.6	7257.7(2)	7257.7	0.027(7)
2063.6	7262.7(3)	7262.7	0.019(5)
2031.5	7294.8(4)	7294.8	0.014(5)
2016.4	7309.9(4)	7309.9	0.014(5)
1986.9	7339.4(5)	7339.4	0.010(4)
1980.4	7345.9(2)	7345.9	0.016(5)
1973.2	7353.1(3)	5027.2	0.023(7)
1962.8	7363.5(4)	7363.5	0.014(4)
		6133.8	0.023(7)
		5605.2	0.018(6)
1953.5	7372.8(4)	6143.1	0.020(7)
1928.7	7397.6(3)	7397.6	0.011(4)
1892.4	7433.9(3)	7433.9	0.013(4)
1877.9	7448.4(4)	7448.4	0.011(4)
1850.2	7476.1(3)	5717.8	0.022(6)
1834.6	7491.7(4)	7491.7	0.010(4)
1829.1	7497.2(4)	7497.2	0.013(4)
1803.1	7523.2(4)	7523.2	0.011(4)
1797.6	7528.7(4)	7528.7	0.010(4)
1771.2	7555.1(3)	5796.8	0.019(6)
1767.8	7558.5(4)	7558.5	0.010(4)
1731.1	7595.2(3)	7595.2	0.013(4)
1707.6	7618.7(2)	5292.8	0.038(7)
1690.3	7636.0(1)	5310.1	0.058(7)
1674.1	7652.2(3)	4914.2	0.030(9)
1447.5	7878.8(3)	7878.8	0.010(4)
1198.0	8128.3(3)	8128.3	0.006(2)
1166.4	8159.9(1)	6117.0	0.026(4)

1. The lower estimation of $i_{\gamma\gamma}$ for cascades with $E_1 < 520 \text{ keV}$ or $E_2 < 520 \text{ keV}$.
2. Only statistical uncertainty of determination of energy and intensity.

Table 2.

The energies E_γ and absolute intensities (% per decay) i_1 of the most intense transitions used for normalization of the cascade intensities in ^{118}Sn . $\sum i_{\gamma\gamma}$ is the observed intensity of the cascades with corresponding primary transition.

E_1 , keV	i_1 [5]	$\sum i_{\gamma\gamma}$
8096.37(17)	0.23(3)	0.37(2)
7268.84(13)	0.40(3)	0.44(1)
6997.7(4)	0.37(8)	0.31(2)
6648.52(7)	1.00(6)	0.75(3)
6422.14(11)	1.04(9)	0.88(4)
6110.0(2)	0.99(2)	0.80(3)
6055.66(18)	0.52(2)	0.55(3)
5444.9(3)	0.55(7)	0.35(1)
5298.1(5)	0.33(5)	0.28(1)
5217.51(10)	0.95(6)	0.60(3)
5208.7(2)	1.1(1)	1.09(4)
4781.55(16)	0.79(6)	0.28(2)
4765.99(15)	0.80(5)	0.51(3)
4556.31(14)	1.33(6)	0.39(4)
Sum	9.85(21)	7.6(1)

Table 3. Energies $E_1 + E_2$ of cascades and their absolute intensities $I_{\gamma\gamma}$ (% per decay). E_f is the energy of the cascade final level

$E_1 + E_2$, keV	E_f , keV	$I_{\gamma\gamma}^{exp}$	$I_{\gamma\gamma}^{mod}$
9326.30	0	16.0(34)	6.7
8096.63	1230	15.3(11)	7.2
7568.00	1758	2.4(7)	1.1
7283.42	2042	3.3(16)	2.4
7269.39	2057	2.8(9)	0.8
7000.36	2325+2328	5.6(9)	2.8
6923.08	2403	2.8(2)	1.5
6829.42	2497	[2]	0.5
6648.95	2677	[1.5]	1.0
6588.29	2738	[4]	1.7
sum		55.8(43)	25.7

Note: intensity of the cascades to the levels $E_f = 2497$, 2677 and 2738 keV was estimated from a comparison of their peak areas in the sum coincidence spectrum with the peak area corresponding to the cascades to the levels 2325 and 2328 keV.

References

- [1] J. Honzátko et al., Nucl. Instr. and Meth. **A376** (1996) 434
- [2] A.M. Sukhovoij and V.A. Khitrov, Sov. J.: Prib. Tekhn. Eksp. **5** (1984) 27
- [3] Yu.P. Popov, A.M. Sukhovoij, V.A. Khitrov and Yu.S. Yazvitsky, Izv. AN SSSR, Ser. Fiz. **48** (1984) 1830
- [4] S.T. Boneva, E.V. Vasilieva and A.M. Sukhovoij, Izv. RAN., Ser. Fiz., **51(11)** (1989) 2023
- [5] Yu.E. Loginov, L.M. Smotritskij, P.A. Sushkov, Vopr. Atom. Nauki i Tech., ser. Fiz. Yad. Reac. (in Russian), **1/2** (2001) 72
- [6] W. Dilg, W. Schantl, H. Vonach and M. Uhl, Nucl. Phys. **A217** (1973) 269
- [7] S.G. Kadenskij, V.P. Markushev and W.I. Furman, Sov. J. Nucl. Phys. **37** (1983) 165
- [8] K. Kitao, Nucl. Data Sheets, **75(1)** (1995) 99
<http://www.nndc.bnl.gov/nndc/nsr/nsrframe.html>
- [9] C.F. Porter and R.G. Thomas, Phys. Rev. 1956. **104**, (1956) 483
- [10] A.M.Sukhovoij and V.A. Khitrov, Physics of Atomic Nuclei, **62(1)** (1999) 19
- [11] E.V. Vasilieva, A.M.Sukhovoij and V.A. Khitrov, Physics of Atomic Nuclei, **64(2)** (2001) 153
- [12] I.Tomandl, V.Bondarenko, D.Bucurescu, J.Honzátko, T.von Egidy, H.-F.Wirth, G.Graw, R. Hertenberger, A.Metz, Y.Eiserman, Proc. 10 International Symposium on Capture gamma-ray spectroscopy and related topics, Santa Fe, USA, Ed. by S.Wender, AIP, (1999) 200
- [13] L.A. Malov and V.G. Soloviev, Yad. Fiz., **26(4)** (1977) 729
- [14] A.M. Sukhovoij and V.A. Khitrov, Bulletin of the Russian Academy of Sciences, Physics **61(11)** (1997) 1611
- [15] E.V. Vasilieva et al., Bulletin of the Russian Academy of Sciences, Physics **57** (1993) 1582

Received on April 28, 2003.

Гонзатко Я. и др.
Интенсивные двухквантовые каскады
и схема гамма-распада составного ядра ^{118}Sn

E3-2003-88

Измерены энергии переходов и интенсивности 454 двухквантовых каскадов при захвате тепловых нейтронов в ^{117}Sn . Эти данные позволили получить более точную и полную схему распада ядра ^{118}Sn .

Автокорреляционный анализ спектра возбужденных промежуточных уровней каскадов позволил определить наиболее вероятный период их эквидистантности. Соответствующий анализ показал невозможность количественного воспроизведения полной интенсивности каскадов в случае учета возбуждений только фермионного типа. Это ведет к заключению, что возбуждение вероятных вибрационных уровней в ^{118}Sn существенно влияет на процесс каскадного гамма-распада этого ядра практически до энергии связи нейтрона B_n .

Работа выполнена в Лаборатории нейтронной физики им. И. М. Франка ОИЯИ.

Препринт Объединенного института ядерных исследований. Дубна, 2003

Honzátko J. et al.
Intense Two-Step Cascades and γ -Decay Scheme
of the ^{118}Sn Compound Nucleus

E3-2003-88

Transition energies and intensities of 454 two-step cascades following thermal neutron capture in ^{117}Sn have been measured. These data allowed us to make more precise and considerably extend the earlier obtained decay scheme of the ^{118}Sn nucleus.

Autocorrelation analysis of the excitation spectrum of intermediate levels of the most intense cascades allowed us to determine the most probable period of their regularity. Besides, analysis showed impossibility to quantitatively reproduce the total cascade intensity with accounting only for the excitations of fermion type. From this resulted the conclusion that the excitations of a probable vibrational type in ^{118}Sn also considerably influence the cascade γ -decay process practically up to the neutron binding energy B_n .

The investigation has been performed at the Frank Laboratory of Neutron Physics, JINR.

Preprint of the Joint Institute for Nuclear Research. Dubna, 2003

Редактор *А. А. Честухина*
Макет *Е. В. Сабоевой*

Подписано в печать 26.05.2003.
Формат 60 × 90/16. Бумага офсетная. Печать офсетная.
Усл. печ. л. 1,31. Уч.-изд. л. 2,01. Тираж 290 экз. Заказ № 53916.

Издательский отдел Объединенного института ядерных исследований
141980, г. Дубна, Московская обл., ул. Жолио-Кюри, 6.
E-mail: publish@pds.jinr.ru
www.jinr.ru/publish/